ISSN 1392–1320 MATERIALS SCIENCE (MEDŽIAGOTYRA). Vol. 19, No. 2. 2013

Influence of Hydrothermal Synthesis Condition on Xonotlite Crystal Morphology

Edmundas SPUDULIS *, Viktoras ŠAVAREIKA, Algimantas ŠPOKAUSKAS

Scientific Institute of Thermal Insulation, Vilnius Gediminas Technical University, Linkmenų 28, LT-08217 Vilnius, Lithuania

crossref http://dx.doi.org/10.5755/j01.ms.19.2.4437

Received 21 June 2011; accepted 15 February 2012

This investigation was made to examine how the conditions of hydrothermal synthesis influence the crystal structure of xonotlite and its morphology. For synthesis we used amorphous silica fume and SiO_2/CaO molar ratio equal to 1.0, water-solids ratio W/S = 10 and W/S = 15. The samples were cured hydrothermally in the rotation autoclave with mixing rod for 2 and 4 hours at 200 °C. The products were characterized by X-ray diffraction, differential thermal analysis, thermogravimetry, SEM, atomic force microscopy and mercury intrusion porosimetry. The low W/S ratio and mixing intensity had a decisive effect on processes of formation of xonotlite. During the 4-hour synthesis at W/S = 15, well formed xonotlite fiber of 0.2 μm diameter was obtained. Under the same conditions, but at W/S = 10, the obtained xonotlite was poorly formed, with fiber of 0.07 μm diameter. The mercury intrusion porosimetry method was used to examine and compare the surface of synthesized xonotlite. In the case of well formed xonotlite, the surface equals to 8.027 m^2/g and that of poorly formed xonotlite 22.328 m^2/g. The investigation of pressed xonotlite powder by XRD shows the rise in diffraction peak intensity (0.700; 0.324) nm and the drop in diffraction peak intensity (0.308; 0.184) nm. With tobermorite, there is a rise in diffraction peak intensity (1.13; 0.542) nm.

Keywords: xonotlite, morphology, water-solids ratio, X-ray diffraction, atomic force microscope, SEM, mercury intrusion porosimetry.

1. INTRODUCTION

The synthesis of calcium hydrosilicate xonotlite $Ca_6Si_6O_{17}(OH)$, in the system CaO-SiO_2-H_2O is so far an important field of research. Xonotlite is synthesized out of various raw materials, which contain CaO and SiO_2, by processing them hydrothermally at temperature of 200 °C – 300 °C [1 – 5]. H. F. W. Taylor [6] stated that the formation of xonotlite is proceeding via intermediate stages where C-S-H (II), C-S-H (I) and tobermorite are generated in turn. Shaw S. [7] showed that at the beginning of synthesis always gel-like C-S-H are forming. Nevertheless, the studies of Japan scientists, which were performed at introduction of xonotlite continuous synthesis technology [8, 9], demonstrated that a swift rise in temperature does not allow for forming C-S-H (II), C-S-H (I) and germs of tobermorite crystals and that xonotlite was crystallized without formation of any solid intermediate compounds. The authors established that the process of synthesis of xonotlite in continuous manner was not influenced by raw materials ratio C/S and admixtures in raw materials. The main product received by this method is xonotlite. However, such method of xonotlite synthesis is possible only at W/S ratio of 200 – 1000.

The duration, dispersity of silicon dioxide used for synthesis and temperature of synthesis are also subject to xonotlite crystalline structure. After exposure of suspension (made of SiO_2 powder and lime milk) for 4 h at temperature of 191 °C, the product of interaction is tobermorite and xonotlite. If the duration of isothermal exposure is 6 h – 8 h, tobermorite fully changes into xonotlite. It is maintained that with ground quartz (particles sized 10 μm – 20 μm), it is possible to synthesize xonotlite out of raw materials at C/S = (0.8 – 1.0) at temperature of 250 °C only [10]. It is as well recommended to grind quartz up to comparative surface of 10000 cm^2/g (according to Blain) or up to particle size of (2 – 25) μm and to synthesize xonotlite at temperature of (191 – 250) °C at W/S ratio of suspension (20 – 35). The crystals of xonotlite synthesized out of dispersive waste silicon dioxide usually are better crystallized than those obtained with use of quartz [11]. What concerns the morphology of crystals, there was an increase in crystal size with increasing temperature, but this led to some crystal damage. Longer hydrothermal treatment, however, leads to more perfect crystal morphologies [12]. The synthesis of xonotlite also depends on state of used lime component. The data are provided to say that the formation of xonotlite is more rapid when CaO is used. Hydrated lime suspension slows down remarkably the formation of xonotlite, the other conditions being alike [13].

At synthesis of xonotlite by dynamic hydrothermal process [14], the authors suggest the continuous mixing of suspension at speed of up to 200 min^{-1}. The proper water-solids ratio is in the range of 28 to 30, the reaction temperature of 220 °C to 225 °C, the reaction time from 6 to 8 hours. The received micro-porous spherical particles of calcium silicate are ranging in size from several microns to hundred microns. It is stressed that the stirring during processing is a key factor for the successful synthesis of spherical xonotlite particles.

Analyzing the information provided, it's obvious that the synthesis of xonotlite is performed at rather high water content (W/S = 20 – 35 for periodic synthesis and W/S = 100 – 200 for continuous synthesis). The high W/S

*Corresponding author. Tel.: +370-5-2753305; fax.: +370-5-2753305.
E-mail address: *edmundas.spudulis@vgtu.lt* (E. Spudulis)

ratio is used for stimulation of solution of silicate component and for more rapid formation of xonotlite, however, this is related to high energy inputs and low efficiency of equipment for hydrothermal processing.

The data showing how the intensity of mixing of suspension influences the kinetics of xonotlite synthesis are not numerous. Most of them specify that suspension is stirred by mixer of certain rotations and in these investigations the ratio W/S is not lower than 25. During the synthesis of calcium hydrosilicates, the reduction of W/S of suspension is restricted by ever growing viscosity of suspension where along with slowly rising temperature, gel-like products are generating and high-speed mixers are not able to mix the cured mass.

The aim of this paper: to establish how the decrease in W/S of suspension (down to 15 and 10) and the intensity of mixing influence the synthesis of xonotlite and the morphology of crystals of the product obtained.

2. MATERIALS AND TEST METHODS

For investigations, the following materials were used: silica fume "Elkem Microsilica 983" of high purity, with the following chemical composition: SiO_2 – 98 %, C – 0.4 %, Fe_2O_3 – 0.05 %, Al_2O_3 – 0.30 %, CaO – 0.3 %, C – 0.4 % , Na_2O – 0.1 %, SO_3 – 0.2 %; chemically pure CaO additionally burned at 950 °C for 4 h.

The molar ratio of the mixture of materials used in all syntheses was the following: C/S = 1 (C – CaO, S – SiO_2). For preparation of suspensions, distilled water was used, water solid ratio 10 and 15. The hydrothermal syntheses were performed by laboratory rotation autoclave of volume 3 dm^3, inner diameter 100 mm, rotation speed 20 rpm. The temperature was raised from 20 °C to 200 °C by speed of 1.5 °C/min, isothermal exposure of 2 h or 4 h. For modeling various intensities of stirring, rods of different diameter and weight were put into the autoclave: ∅ 5 mm – 132 g, ∅ 8 – 170 g, ∅ 10 mm – 267 g. To the aim of determining whether the rod performs functions of stirring and crushing or only that of stirring, bushes were pulled over rods not to let them touch walls of autoclave, but to do the stirring of suspension only.

The X-ray diffraction analysis of synthesis products was performed by apparatus DRON-7 and DRON-2. In the first case Cu K_α radiation was used and Ni filter, in the second case Co K_α radiation and Fe filter. The differential thermal analysis (DTA) and thermogravimetric analysis (TG) performed by thermograph Linseys STA 1600, the weight of samples being 70 mg, platinum crucibles, temperature rise speed of 15 °C/min, inert material Al_2O_3, air medium. The surface image of sample from xonolitle powder pressed at 100 MPa was tested by atomic force microscope DUALSCOPE^{TM} DS 45. The structure of pores in samples was investigated by a mercury porosimeter "Quantachrome Poremaster" (33/60). The distribution of suspended particles by size was determined by laser particle size analyzer CILAS 1090 with optical microscope. The morphology of synthesized materials was investigated by a scanning electron microscope JEOL JSM-7600F.

3. RESULTS AND DISCUSSION

The conditions of xonotlite synthesis performed during this investigation and the state of suspension after synthesis are provided in Table 1.

The XRD tests were performed with obtained products of synthesis to determine the main phases. The data are provided in Figs. 1 and 2. It was established that during the syntheses S1 and S2 the components did not react fully, as there are diffraction peaks of free lime (0.491; 0.263) nm. Other peaks can be allocated to calcium hydrosilicates of type C-S-H (II) ir C-S-H (I). However, in the sample S2 there are peaks (0.700; 0.362) nm, which can be allocated to germs of xonotlite, since they have no clear signs of tobermorite. Upon increase in exposure time of syntheses S3 and S4 up to 4 h, xonotlite is mainly received with diffraction peaks (0.700; 0.425; 0.362; 0.323; 0.308; 0.282; 0.270; 0.251; 0.203; 0.195; 0.184) nm.

The sample of synthesis S3 contains tobermorite (peak 1.13 nm), meanwhile it is not observable in the sample of synthesis S4. The obtained data show that at W/S = 10, even slightly increasing the intensity of stirring during the synthesis of calcium hydrosilicates, one can considerably influence the compositions of new formations, and the received suspensions are fluid.

The XRD investigations of samples show that along with increase in W/S of suspensions up to 15 after 4-hour isothermal exposure even without use of a stirring body (Synthesis S5), xonotlite of high crystalline degree was received. The same result is obtained using a stirring rod with bushes for stirring of suspension only. The xonotlite

Table 1. Conditions of calcium hydrosilicates syntheses.

Synthesis code	Ratio W/S	Duration of isothermal exposure, h	Data of mixing rod	State of suspension after synthesis
S1	10	2	∅ 10 mm	Thin suspension. No grains.
S2	10	2	∅ 5 mm, 2 pieces	Rapid stratification of suspension is observed.
S3	10	4	∅ 8 mm	Rapid stratification of suspension is observed.
S4	10	4	∅ 10 mm	Thin suspension. No grains.
S5	15	4	Not available	The material is accumulated at the bottom of reactor. The material contains grains.
S6	15	4	∅ 10 mm, with bushes	The material contains grains (less than in S5).
S7	15	4	∅ 10 mm	Thin suspension. No grains.

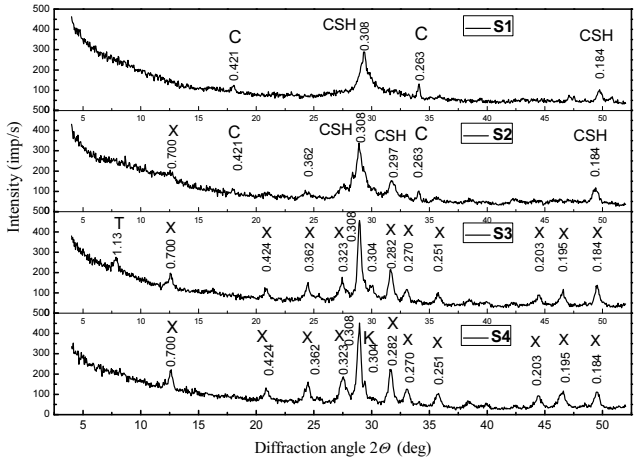

Fig. 1. XRD patterns of products synthesized at W/S = 10 (S1, S2, S3, S4) (X- xonotlite, T – tobermorite, C – lime)

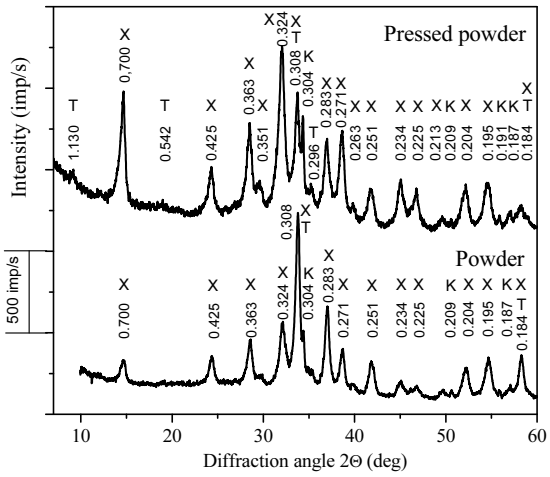

Fig. 3. XRD paterns of S4 powder sample and pressed powder sample (W/S = 10) (X – xonotlite, T – tobermorite, K – calcite)

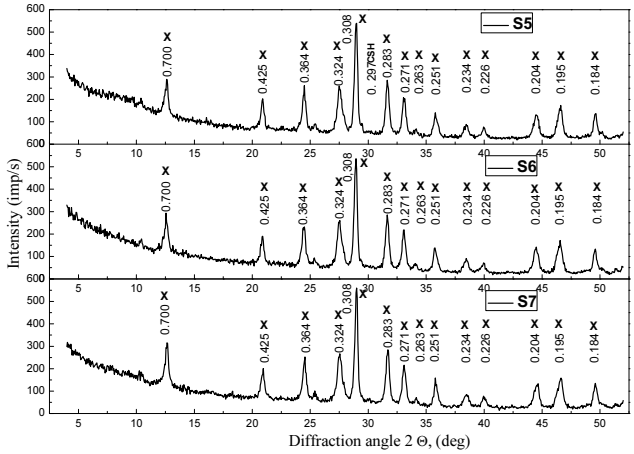

Fig. 2. XRD patterns of products synthesized at W/S = 15, (S5, S6, S7) (X – xonotlite)

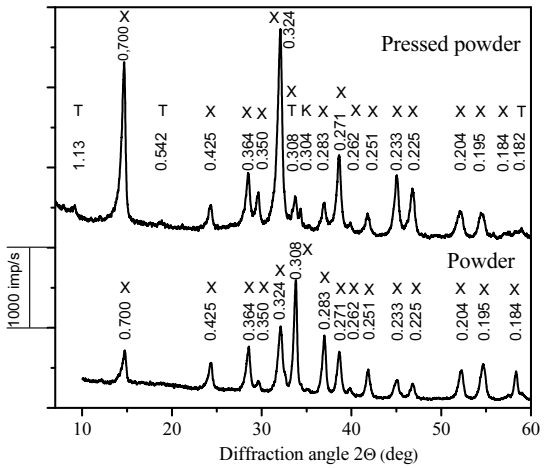

Fig. 4. XRD paterns of S7 powder sample and pressed powder sample (W/S = 15) (X – xonotlite, T – tobermorite, K – calcite)

suspension of the lowest viscosity was received during the synthesis S7 using the heaviest rod. It was established that even at slow rise of temperature in the rotation autoclave with mixing rods, 4-hour isothermal exposure, temperature of 200 °C and temperature rise of 1.5 °C/min., it is possible to synthesize xonotlite of high crystalline degree.

By pressing anisotropic crystals, they often are compacted in such way that their main planes become parallel and XRD data are approximating to those of ideal crystal. Such investigation was performed with the samples S4 and S7 in order to find out how the ratio W/S influences differences in their crystalline structure. As it can be seen from the XRD patterns of powder samples S4 and S7 (Figs. 3 and 4), the main compound observable in both cases is xonotlite.

However, the peaks of xonotlite in the sample S4 are wider and the received signal is relatively much weaker. In this sample the peaks of calcite (0.304; 0.209) nm are observable, while some other peaks can be allocated to tobermorite (0.308; 0.184) nm. The XRD patterns for samples pressed under pressure of 50 MPa are provided on the top of Fig. 3 and Fig. 4. Judging from changes in intensity of peaks both samples are anisotropic and fibrous. In both pressed samples, due to orientation of crystals, the peak of xonotlite 0.324 nm is prominent. Nevertheless, beside xonotlite, the peaks of anisotropic tobermorite crystals are well seen: in the sample S4 (1.13; 0.542; 0.296) nm and in the sample S7 (1.13; 0.542) nm. The peak 0.182 nm in the sample S7 witnesses about formation of calcium hydrosilicates with the ratio C/S lower than 1.

The fact that calcium hydrosilicates synthesized under same conditions except for different W/S differ in their composition is confirmed as well by the data of thermal analysis for the samples S4 and S7, which are provided in Fig. 5. In DTA pattern 1.2 for the sample S4, the effect of endothermal adsorbed water removal is observable at temperatures from 20 °C to 360 °C, while at 494 °C observe a slight effect of endothermal water removal from larger calcium hydrosilicates crystals. Starting from 680 °C the endothermal water removal effect with the highest speed of disintegration at 747.7 °C is observed. The presence of not only xonotlite, but also of tobermorite in the sample S4 is shown by exothermal effect of crystallization of wollastonite with its maximum at 810.5 °C. The DTA

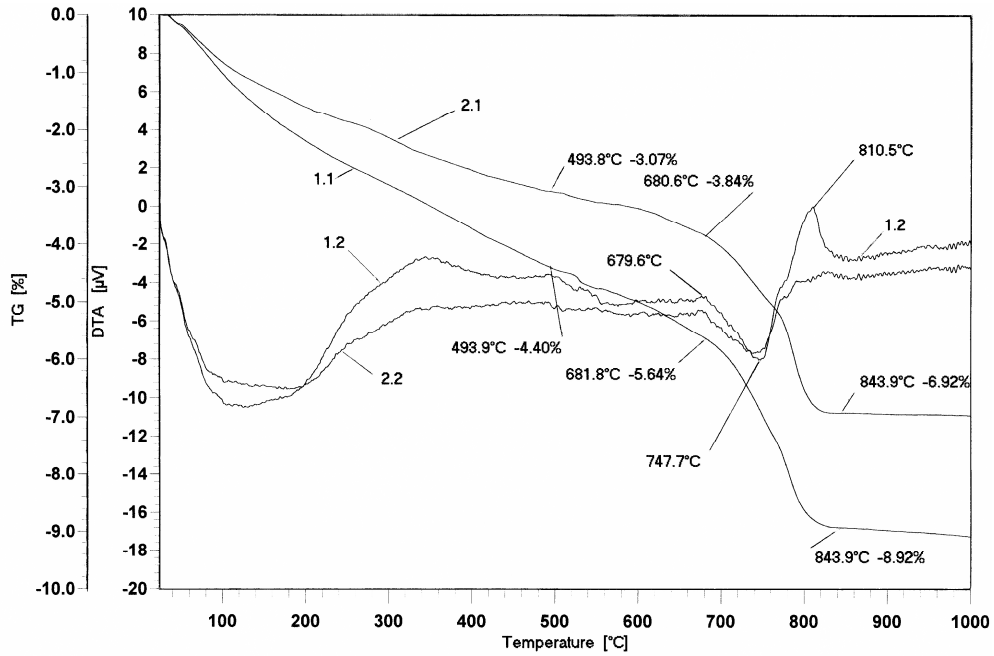

Fig. 5. Data of thermal analysis for the samples S4 and S7: 1.1 – S4 sample TG ,%; 2.1– S7 sample TG ,%; 1.2 – S4 sample DTA; 2.2– S7 sample DTA

pattern of sample S7 differs but little, there is no effect of crystallization of wollastonite, as xonotlite changes into wollastonite topotactically. At temperature of up to 844 °C, the total mass loss in the sample S4 makes 8.92 %, and in S7 6.92 %. This loss caused by heating is composed of discharged water and CO_2.

Using the optical microscope at CILAS 1090, it was established (Figs. 6 and 7) that the suspensions of xonotlite samples S4 and S7 consist of fibrous crystal agglomerates. The distribution of synthesized xonotlite crystal agglomerates by size in suspension was determined by laser particle size analyzer. The distribution of particles by size in the samples S4 and S7 is provided in Figs. 8 and 9.

The distribution of particles by size show that the diameters of agglomerates are marginally influenced by the conditions of synthesis, though in the sample S7 they are slightly higher.

The remarkable differences in the morphology of xonotlite crystals of samples S4 and S7 are observable by SEM. It appears that after drying of suspensions, the crystals of xonotlite make spherical agglomerates (Figs. 10 and 11), and the diameter of which corresponds to those determined by particle size analyzer. However, there are the essential differences. The surface of agglomerates of sample S4 is smooth, while that of S7 is fluffed up. The cause of this phenomenon is an extremely differing size of crystals in the samples S4 and S7, as visible in Figs. 12 and 13.

The fibers of crystals of sample S4 are thin, 3 μm – 6 μm long, while those of sample S7 are much thicker, length of 6 μm – 12 μm. The authors [14] indicate that spherical particles from xonotlite are received by them at ratio W/S 30 only. Nevertheless, the data provided there show that spherical agglomerates are generating at ratio W/S 10 – 15 as well. But in the latter case the ratio W/S exerts a much more considerable effect on morphology of synthesized xonotlite crystals.

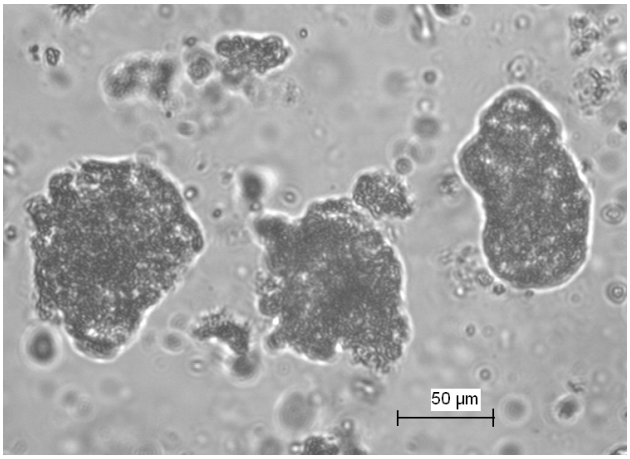

Fig. 6. Image of xonotlite crystal agglomerates in suspension, the sample S4

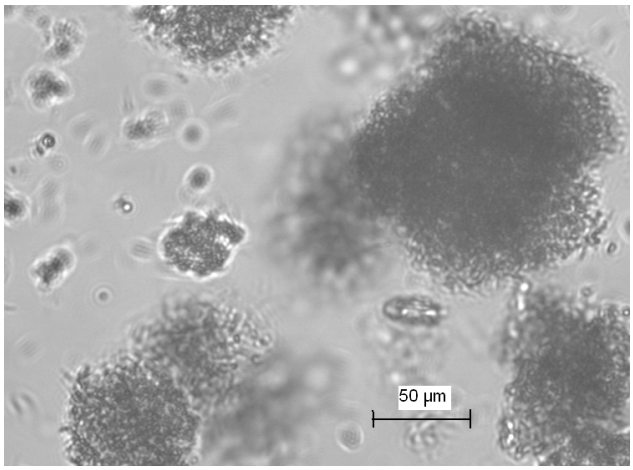

Fig. 7. Image of xonotlite crystal agglomerates in suspension, the sample S7

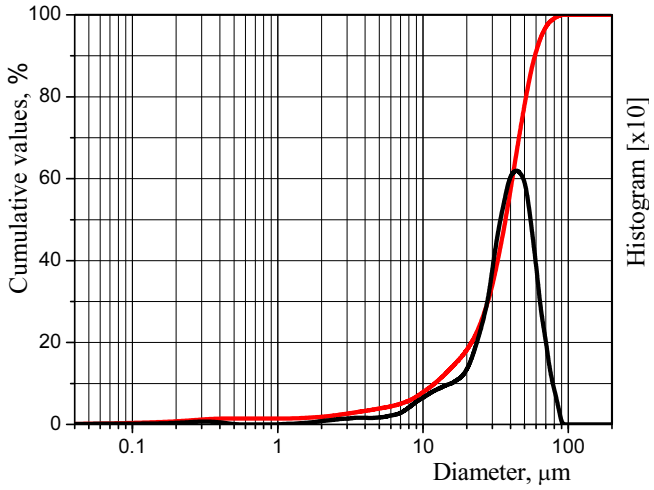

Fig. 8. Distribution of agglomerates by size in suspension of sample S4

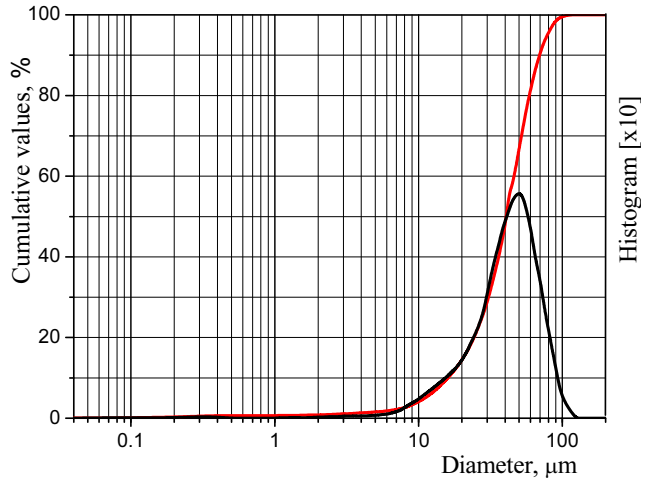

Fig. 9. Distribution of agglomerates by size in suspension of sample S7

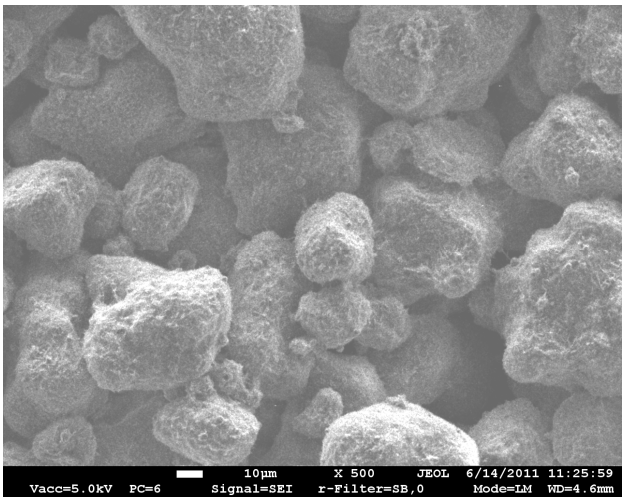

Fig. 10. SEM image of S4 sample, magnification ×500

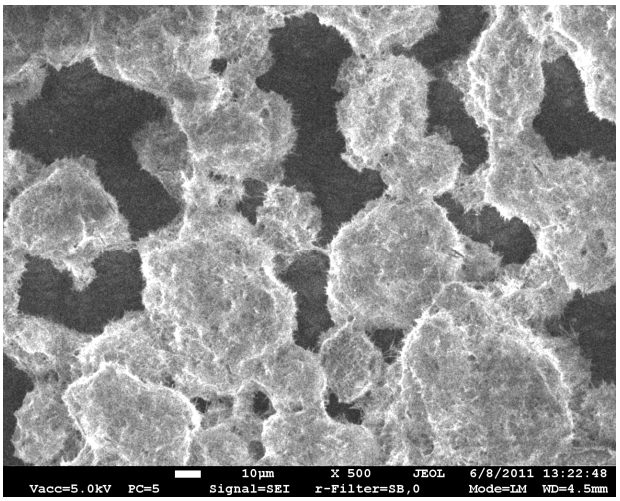

Fig. 11. SEM image of S7 sample, magnification ×500

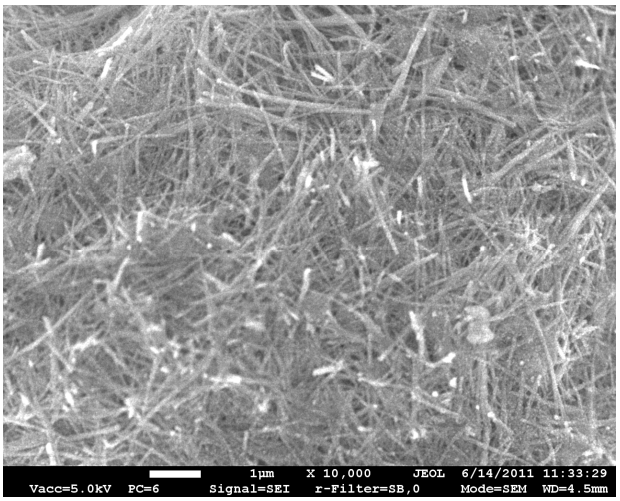

Fig. 12. SEM image of S4 sample, magnification ×10000

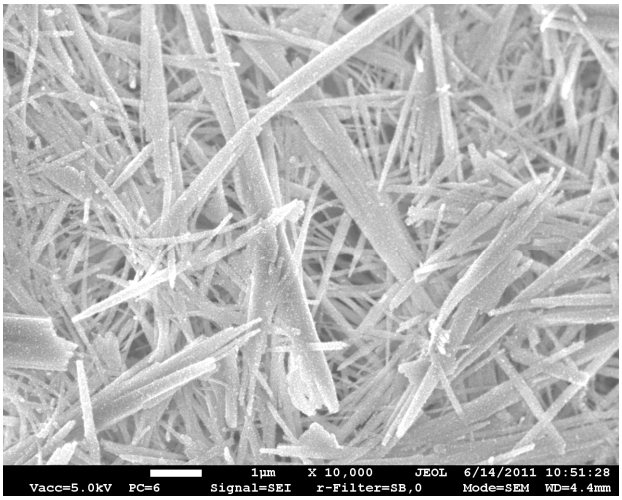

Fig. 13. SEM image of S7 sample, magnification ×10000

The impact of W/S value on morphology of synthesized xonotlite was investigated by atomic force microscope. The samples S4 and S7 were pressed by force of 100 MPa using the equipment with polished surfaces. The images of received surfaces are provided in Figs. 14 and 15. By means of atomic force microscope the areas of 1.02 μm × 1.02 μm were scanned. The surface of sample S4 is formed out of 18 – 20 parallel stripes, which can be regarded as surface of separate fibers. The surface of sample S7 is formed out of 5 – 6 parallel larger straight crystals. The diameters of synthesized fibrous crystals can be determined by given cross sections of received surfaces (Figs. 16 and 17). According to the data of cross sections, the diameter of S4 xonotlite equals to 0.07 μm, S7 – 0.2 μm.

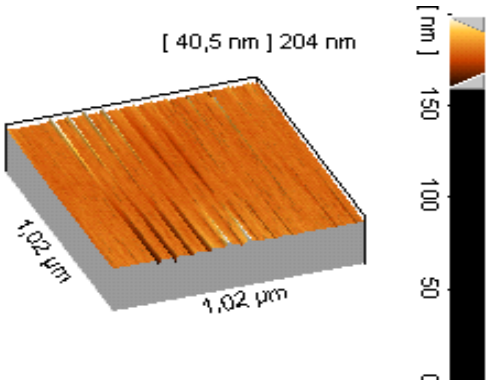

Fig. 14. Atomic force microscope image of surface of sample S4. *Height of sample (204 nm) and height of surface irregularities (40.5 nm) is shown on the right side of figure

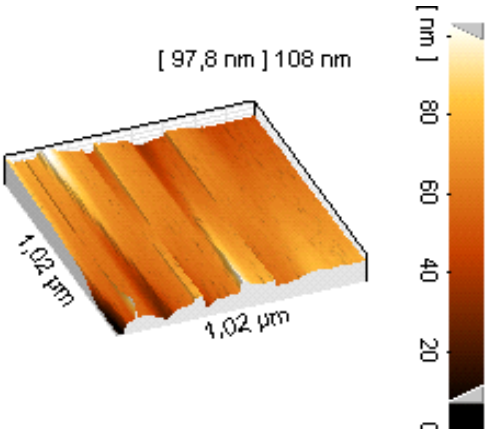

Fig. 15. Atomic force microscope image of surface of sample S7. *Height of sample (108 nm) and height of surface irregularities (97.8 nm) is shown on the right side of figure

Subject to size of synthesized crystals, the structure of pores of material is changing as well. The pore structure of samples S4 and S7 was investigated by mercury porosimetry. The pore structure of powder can be described both by pores between crystals and inner pores. Nonetheless, these sizes for powder-like materials depend in particular on their compacting. By the way, the size of pores between crystals is not informative. The data of mercury porosimetry enable to find out the comparative surfaces of material and the relationship between comparative surfaces and pore diameters. Since the comparative surface of material is extremely subject to number of low-diameter pores, in this way we can evaluate the morphological differences of synthesized materials. The relationship between surface area and pore diameter in the samples S4 and S7 is provided in Fig. 18.

Fig. 16. Profile of cross section of sample S4

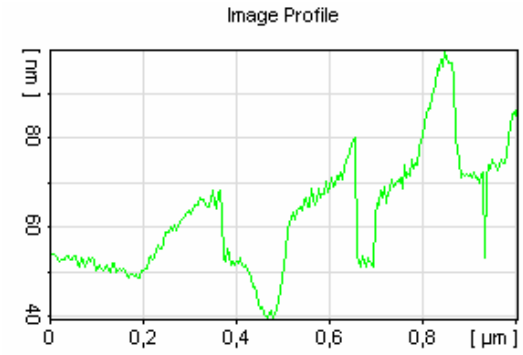

Fig. 17. Profile of cross section of sample S7

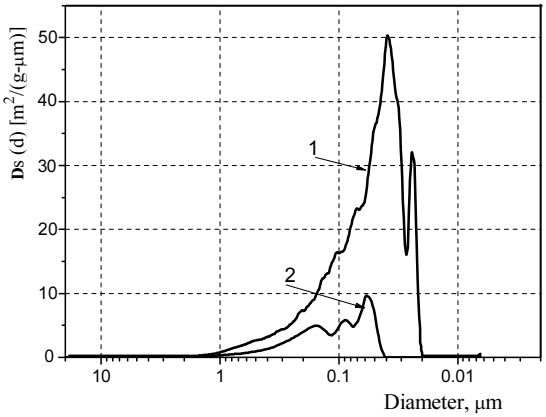

Fig. 18. Relationship between pore surface area and pore diameter in synthesized samples: 1 – sample S4, 2 – sample S7

It was established that the total surface area of pores between crystals in the sample S4 equals to 23.328 m^2/g, and in S7 to 8.027 m^2/g. The received data about surface area of pores in the samples confirm the SEM and atomic force microscope data about morphology of xonotlite crystals and allow for evaluating the properties of synthesized products in numbers. Interpreting the data from Fig. 18 and knowing that the samples are composed of fibrous crystals and that the measured surface is the surface of pores between fibrous crystals (what indirectly describes the surface of fibrous crystals), it may be

concidered that the sample S4 consists of smaller crystals with greater surface and that it contains pores of some characteristic diameters and fibrous crystals of some characteristic diameters (Curve 1). The crystals of sample S7 are larger and make pores of considerably smaller surface area, however, here crystals of some characteristic diameters can also be observed (see Curve 2, Fig. 18).

4. CONCLUSIONS

It was established that it is possible to synthesize xonotlite with high crystalline degree at W/S 10 or 15. However, the W/S value influences considerably the morphology of synthesized xonotlite. Using amorphous silica fume when the molar ratio of CaO/SiO_2 equals to 1 and stirring the suspension of W/S = 15 in the rotation autoclave with rod-shaped mixing bodies, it is possible to synthesize hydrothermally in 4 h at 200 °C xonotlite of high crystalline degree. Under the same conditions, xonotlite with admixture of tobermorite can be received when W/S = 10. At W/S = 10 and W/S = 15, the diameters of fibers in the synthesized xonotlite samples are 0.07 μm and 0.2 μm and their length is 3 μm – 6 μm and 6 μm – 12 μm, respectively. When W/S = (10 – 15), during synthesis the fibrous crystals of xonotlite form agglomerates sized (10 – 100) μm diameter. These agglomerates retain their shape in suspension after drying.

REFERENCES

1. **Schlegel, E., Strienitz, R.** Faserfärmige Kalzium-silikathydrate *Silikattechnik* 41 (8) 1990: pp. 278 – 283.
2. **Ono, M., Yoshii, K., Kuroki, T., Yamasaki, N., Tsunematsu, S., Bignall, G.** Development of Porous Silica Production by Hydrothermal Method *High Pressure Research* 10 2001: pp. 307 – 310. http://dx.doi.org/10.1080/08957950108206178
3. **Qiju, Z., Wang, W.** Calcium Silicate Based High Efficienccy Thermal Insulation *British Ceramic Transaction* 99 (4) 2000: pp. 187 – 190. http://dx.doi.org/10.1179/096797800680929
4. **Liu, F., Zeng, L., Cao, J., Li, J.** Preparation of Ultra-light Xonotlite Thermal Insulation Material Using Carbide Slag *Journal of Wuhan University of Technology-Mater* April 2010: pp. 295 – 297.
5. **Fei, L., Ling, K. Z., Jian, X. C., Bo, Z. A. Y.** Hydrothermal Synthesis of Xonotlite Fibers and Investigation on their Thermal Property *Chinese Ceramics Communications. Advanced Materials Research* 105 – 106 2010: pp. 841 – 843.
6. **Taylor, H. F. W.** Cement Chemistry. San Diego DA: Academic Press, 1997: 459 p. http://dx.doi.org/10.1680/cc.25929
7. **Shaw, S., Clark, S. M., Henderson, C. M. B.** Hydrothermal Formation of Calcium Silicate Hydrates, Tobermorite ($Ca_5Si_6O_{16}(OH)_2$ $4H_2O$) and Xonotlite ($Ca_6Si_6O_{17}$ $(OH)_2$): An in situ Synchrotron Study *Chemical Geology* 167 (1 – 2) 2000 pp. 129 – 140.
8. **Yanagisawa, K., Feng, Q., Yamasaki, N.** Hydrothermal Synthesis of Xonotlite Whiskers by Ion Diffusion *Journal of Materials Science Letters* 16 1997: pp. 889 – 891. http://dx.doi.org/10.1023/A:1018575702546
9. **Yanagisawa, K., Sun, E., Feng, Q.** Continuous Synthesis of Xonotlite by hydrothermal reaction *Journal of the Society of Inorganic Materials, Japan* 10 (303) 2003: pp. 110 – 114.
10. **Alujević, V., Bejzak, A., Glasnović, A.** Kinetic Study of the Hydrothermal Reaction in CaO-Quartz System *Cement and Concrete Research* 16 (5) 1986: pp. 695 – 699. http://dx.doi.org/10.1016/0008-8846(86)90043-8
11. **Kurbus, B., Bakula, F., Gabrovšek, R.** Reactivity of SiO_2 Fume from Ferrosilicon Production with $Ca(OH)_2$ Under Hydrothermal Conditions *Cement and Concrete Research* 15 (1) 1985: pp. 134 – 140. http://dx.doi.org/10.1016/0008-8846(85)90018-3
12. **Black, L., Garbev, K., Stumm, A.** Structure, Bonding and Morphology of Hidrothermally Synthesised Xonotlite. http://eprints.whiterose.ac.uk/4750/2/hydrothermal Synthesis of Xonotlite.pdf (viewed: 2011 02 22).
13. **Baltakys, K., Prichockiene, E.** Influence of CaO Reactivity on the Formation of Low-base Calcium Silicate Hydrates *Materials Science-Poland* 28 (1) 2010: pp. 295 – 304.
14. **Li, M., Liang, H.** Formation of Micro-porous Spherical Particles of Calcium Silicate (Xonotlite) in Dynamic Hydrothermal Process *China Particuology* 2 (3) 2004: pp. 124 – 127.

Presented at the 20th International Baltic Conference "Materials Engineering 2011" (Kaunas, Lithuania, October 27–28, 2011)